A biofilm-tropic *Pseudomonas aeruginosa* bacteriophage uses the exopolysaccharide Psl as receptor

Brenna Walton[1)], Serena Abbondante[2,3)], Michaela Ellen Marshall[2,3)], Justyna M. Dobruchowska[4)], Amani Alvi[1)], Larry A. Gallagher[5)], Nikhil Vallikat[1)], Zhemin Zhang[8)], Daniel J. Wozniak[6,7)], Edward W. Yu[8)], Geert-Jan Boons[4,9,10)], Eric Pearlman[2,3)], Arne Rietsch[1,11)]

1) Dept. of Molecular Biology and Microbiology, Case Western Reserve University, Cleveland, OH, U.S.A.
2) Dept. of Ophthalmology, University of California, Irvine, CA, U.S.A.
3) Institute of Immunology, University of California, Irvine, CA, U.S.A.
4) Dept. of Chemical Biology and Drug Discovery, Utrecht Institute for Pharmaceutical Sciences, and Bijvoet Center for Biomolecular Research, Utrecht University, Utrecht, NL
5) Dept. of Microbiology, University of Washington, Seattle, WA, U.S.A.
6) Dept. of Microbial Infection and Immunity, The Ohio State University, Columbus, OH, U.S.A.
7) Dept. of Microbiology, The Ohio State University, Columbus, OH, U.S.A.
8) Dept. of Pharmacology, Case Western Reserve University, Cleveland, OH, U.S.A.
9) Complex Carbohydrate Research Center, University of Georgia, Athens, GA, U.S.A.
10) Dept. of Chemistry, University of Georgia, Athens, GA, U.S.A.
11) Corresponding author: arne.rietsch@case.edu

Abstract

Bacteria in nature can exist in multicellular communities called biofilms. Biofilms also form in the course of many infections. *Pseudomonas aeruginosa* infections frequently involve biofilms, which contribute materially to the difficulty to treat these infections with antibiotic therapy. Many biofilm-related characteristics are controlled by the second messenger, cyclic-di-GMP, which is upregulated on surface contact. Among these factors is the exopolysaccharide Psl, which is a critically important component of the biofilm matrix. Here we describe the discovery of a *P. aeruginosa* bacteriophage, which we have called Clew-1, that directly binds to and uses Psl as a receptor. While this phage does not efficiently infect planktonically growing bacteria, it can disrupt *P. aeruginosa* biofilms and replicate in biofilm bacteria. We further demonstrate that the Clew-1 can reduce the bacterial burden in a mouse model of *P. aeruginosa* keratitis, which is characterized by the formation of a biofilm on the cornea. Due to its reliance on Psl for infection, Clew-1 does not actually form plaques on wild-type bacteria under standard *in vitro* conditions. This argues that our standard isolation procedures likely exclude bacteriophage that are adapted to using biofilm markers for infection. Importantly, the manner in which we isolated Clew-1 can be easily extended to other strains of *P. aeruginosa* and indeed other bacterial species, which will fuel the discovery of other biofilm-tropic bacteriophage and expand their therapeutic use.

42 **Introduction**

43 Biofilms formed by bacteria at sites of infection significantly increase the difficulty of treatment
44 with conventional antibiotic therapy. This increased resistance to antibiotic therapy has been attributed
45 to a variety of factors, including reduced penetration of antibiotics (1, 2), as well as an increase in
46 antibiotic-tolerant persister bacteria (3, 4). Formation of biofilms is a feature of many *P. aeruginosa*
47 infections, including lung infections in cystic fibrosis patients (5, 6), wound, catheter, and device infections
48 (7), as well as blinding corneal infections (8-10). In some instances, these biofilms have been found to
49 be astonishingly antibiotic tolerant (11).

50 In addition to the antibiotic tolerance of bacteria in biofilms, there has been a significant increase
51 in antibiotic resistant isolates (12). In fact, *P. aeruginosa* is one of the particularly worrisome ESKAPE
52 group of pathogens (13). With the general rise of antibiotic-resistant isolates, phage therapy has garnered
53 some interest as an alternative to treat these infections (14, 15). However, biofilm formation frequently
54 interferes with phage infection (16), and even though a few bacteriophage that can target *P. aeruginosa*
55 in a biofilm have been described (17, 18), the mechanism by which they infect these biofilm bacteria is
56 unknown.

57 The extracellular matrix of *P. aeruginosa* biofilms is comprised of exopolysaccharides, including
58 Psl, Pel, and alginate, as well as proteins and DNA (19, 20). Psl is of significant interest, since it is critical
59 for biofilm formation, where it is needed for the initial surface attachment (21), as well as structural stability
60 of the mature biofilm (22). Psl has been detected on the surface of individual *P. aeruginosa* bacteria in
61 an apparent helical pattern (20). It is also deposited on surfaces by a subset of motile explorer bacteria
62 during the early stages of aggregate formation (23). Psl production interferes with complement deposition
63 and neutrophil functions, such as phagocytosis and ROS production (24). Moreover, Psl enhances the
64 intracellular survival of phagocytosed *P. aeruginosa*, as well as survival in mouse models of lung and
65 wound infection (24).

66 Here we describe the discovery of a bacteriophage that uses Psl, this crucial biofilm
67 exopolysaccharide, as a receptor. Interestingly, this bacteriophage only infects a subpopulation of
68 planktonically growing *P.* aeruginosa, but it can disrupt biofilms and replicates efficiently on biofilm-grown

69 bacteria. Moreover, the phage can reduce the bacterial burden in a corneal infection model, which
70 involves formation of a biofilm.
71
72 **Results**
73 **Phage Clew-1 can form plaques on a Δ*fliF* mutant, but not wild type *P. aeruginosa*.**
74 We screened wastewater samples at the three Northeast Ohio Regional Sewer District water
75 treatment plants in Cleveland for bacteriophage. The majority of phage in these samples used type IV
76 pili as a receptor, and we wanted to exclude these from our screen. We had previously generated a Δ*fliF*
77 Δ*pilA* double mutant strain in the lab and decided to use it to exclude both surface appendages as
78 potential receptors. This turned out to be fortuitous, since, surprisingly, the screen identified four phage
79 that could form plaques on the Δ*fliF* Δ*pilA* double mutant strain, but not the parental wild type *P.*
80 *aeruginosa* PAO1. We named these Cleveland wastewater-derived phage Clew-1, -3, -6, and -10.
81 Subsequent tests determined that it was the *fliF* deletion that rendered *P. aeruginosa* permissive for
82 infection by these phages. All four Clew phage can plaque on a *fliF* deletion mutant of *P. aeruginosa*
83 PAO1, but not the corresponding wild-type strain or Δ*pilA* mutant strain. (Fig. 1A, S1A, S1B, S2). An
84 unrelated phage we isolated in the same screen, which uses O-antigen as receptor, was used as a control
85 in these experiments (Our control phage, Ocp-2). The Clew bacteriophages belong to the family of
86 Bruynogheviruses (25) and are all highly related (Fig. 1B, S1C). Morphologically, like other members of
87 the family, they are Podoviruses (Fig. 1C).
88
89 **c-di-GMP levels control infection of *P. aeruginosa* by bacteriophage Clew-1.**
90 We next examined what part of the flagellum is involved in determining sensitivity to the Clew-1
91 phage. Mutations affecting the MS-ring (Δ*fliF*) and associated proteins FliE or FliG (26) resulted in Clew-
92 1 sensitivity. However, mutations in the ATPase complex only conferred partial sensitivity, and mutations
93 affecting the hook or flagellar filament did not result in sensitivity, nor did a mutation that affects the type
94 III secretion function of the flagellar basal body by impeding proton flux, *flhA(R147A)*(27)(Fig. S3). We
95 therefore conclude that it is the presence of the MS-ring and not other aspects of the flagellum, such as
96 assembly of the full flagellar structure or flagellar rotation, that control phage sensitivity.

97 Interestingly, we found that deletion of *fleQ*, which is required for transcription of flagellar genes
98 (28), had a very minor effect on Clew-1 phage susceptibility of the wild-type bacteria, and actually
99 decreased Clew-1 susceptibility of the Δ*fliF* mutant bacteria (Fig. S1E). FleQ is a c-di-GMP-responsive
100 transcription factor that, among other things, reciprocally controls flagellar gene expression and
101 production of biofilm-related characteristics, such as the production of the extracellular polysaccharides
102 Psl and Pel, as well as the adhesin CdrA (28-30). We therefore examined whether manipulating c-di-
103 GMP levels controls phage susceptibility. To this end we produced the c-di-GMP phosphodiesterase
104 PA2133 from a plasmid (31) to artificially lower c-di-GMP levels in the Δ*fliF* deletion mutant. Conversely,
105 we artificially elevated c-di-GMP levels in the wild-type by deleting the *wspF* gene (31). Lowering c-di-
106 GMP levels in the Δ*fliF2* mutant restored Clew-1 resistance (Fig. 1D), whereas deleting *wspF* rendered
107 the parental PAO1 strain phage sensitive (Fig. 1E). Taken together, these data demonstrate that Clew-1
108 susceptibility is controlled by intracellular c-di-GMP levels and argue that absence of the MS-ring controls
109 phage susceptibility through an increase in c-di-GMP.
110
111 **Phage Clew-1 requires Psl for infection.**
112 To better understand the host factors that control susceptibility and resistance to Clew-1 infection,
113 we carried out a pair of TnSeq experiments. In the first of these, we mutagenized the wild-type strain
114 PAO1F with the mini-mariner transposon TnFAC (32), and the resultant mutant library was infected with
115 phage Clew-1 at an MOI of 10 for 2 hours. The surviving bacteria were allowed to grow up after plating
116 on an LB plate and the transposon insertion sites for the input and output pool were determined by
117 Illumina sequencing. We identified insertion mutants that were depleted after infection (Fig. 2A). Two of
118 the genes with the most significant depletion were *fliF* and *fliG*, consistent with our previous analysis
119 indicating that these mutations sensitize PAO1 to Clew-1 infection. Interestingly we also noted depletion
120 of *pch* and *bifA* insertions, both encoding phosphodiesterases that are involved in depleting c-di-GMP in
121 the flagellated daughter cell after cell division (33-36). In fact, *pch* interacts with the chemotactic
122 machinery (33), highlighting, here too, the importance of c-di-GMP in controlling Clew-1 sensitivity.
123 In a reciprocal experiment, we carried out the TnSeq analysis in a *fliF* mutant strain. This analysis
124 identified insertions in the *psl* operon as the most highly enriched group of mutants after Clew-1 selection,

125 suggesting that Psl is required for phage infection (Fig. 2B). We examined the requirement for Psl
126 explicitly by generating *pslC* and *pslD* mutants in the PAO1F Δ*fliF2* strain background. PslC is a
127 glycosyltransferase required for Psl biosynthesis, while PslD is required for Psl export from the cell (37,
128 38). Deletion of either *pslC* or *pslD* rendered the *fliF* mutant bacteria Clew-1 resistant and sensitivity could
129 be restored through complementation using a plasmid-borne copy of the deleted open reading frame
130 (Fig. 2C). These data demonstrate that Psl production is required for infection of *P. aeruginosa* by phage
131 Clew-1.
132
133 **Phage Clew-1 attachment is Psl-dependent**
134 We next examined whether attachment of Clew-1 to *P. aeruginosa* is Psl-dependent. We first used
135 efficiency of center of infection (ECOI) analysis to examine attachment. In this analysis, the phage is
136 allowed to adhere to the bacteria for 5 minutes, before washing the bacteria to remove unattached phage.
137 The bacteria are then diluted, mixed with top agar and a sensitive indicator bacterium (Δ*fliF2*), and then
138 plated to allow for plaque formation as a biological readout of attached bacteriophage. Attachment of
139 phage Clew-1 is Psl-dependent. Interestingly, we were able to detect Psl-dependent attachment both
140 with wild-type and Δ*fliF2* mutant bacteria (Fig. 3A), which contradicted out initial efficiency of plating
141 experiments. We therefore reexamined phage susceptibility by monitoring phage infection in liquid media
142 and generating lysis curves for wild-type and Δ*fliF2* mutant bacteria, as well as their Δ*pslC* mutant
143 derivatives (Fig. S4). The Δ*fliF2* mutant strain was lysed after ~40 minutes of infection. The wild-type
144 bacteria displayed a significant slowing of growth upon Clew-1 infection when compared to the uninfected
145 culture, but not clear lysis as was observed with the Δ*fliF2* mutant. In both instances, deleting *pslC*
146 abolished any phage-dependent effect on growth.
147 We hypothesized that perhaps, the difference between wild-type and Δ*fliF2* mutant bacteria is due
148 to the fraction of cells that are producing Psl and therefore permissive for phage attachment. To test this
149 hypothesis, we labeled phage Clew-1 with the DyLight594 fluorescent dye and examined attachment
150 directly by microscopy (Fig. 3B). We observed a statistically significant increase in the percentage of
151 bacteria with attached bacteriophage in the Δ*fliF2* mutant bacteria compared to the wild-type, arguing
152 that the increase in c-di-GMP in the Δ*fliF2* mutant increases the fraction of Clew-1 susceptible cells in the

153 population. As anticipated, no phage was observed attached to the corresponding Δ*pslC* mutant (Fig.
154 3C).
155
156 **Phage Clew-1 binds to Psl directly**
157 We next examined whether phage Clew-1 can bind to Psl directly. We first determined whether
158 we could precipitate phage Clew-1 from filter sterilized culture supernatants of a Δ*fliF2* mutant using an
159 antibody directed against Psl. The presence of the phage was determined by quantitative PCR. We were
160 able to pull down phage Clew-1 in a Psl and antibody-dependent manner with Δ*fliF2* Δ*pslC* culture
161 supernatants serving as a control (Fig. 4A). Notably, we observed some Psl-dependent attachment in the
162 absence of antibody, arguing that Psl binds non-specifically to the magnetic beads we used in our
163 experiments. Including the anti-Psl antibody resulted in a statistically significant increase compared to
164 this background level of attachment (Fig. 4A). We next repeated the pulldown using a partially purified
165 fraction of cell-associated Psl to repeat the pulldown and again found Psl and antibody dependent
166 precipitation of phage Clew-1 (Fig. S6). Finally, we examined phage binding using a biotinylated, affinity
167 purified preparation of Psl and found that we could pull down the phage using this Psl fraction as well,
168 arguing that Clew-1 binds Psl directly (Fig. 4B).
169
170 **Phage Clew-1 infects wild-type *P. aeruginosa* in biofilms**
171 Since Clew-1 exploits Psl for infection and Psl is a key component of the biofilm matrix of most
172 strains of *P. aeruginosa* (39, 40), we hypothesized that, perhaps, Clew-1 can infect biofilm bacteria. We
173 used a static-biofilm model to test this hypothesis. Biofilms were established overnight in a 96-well plate.
174 One plate was washed and fixed with ethanol to quantify the day one biofilm mass using crystal violet
175 staining. In a second plate, established in parallel, the biofilms were washed with PBS and LB was added
176 back, either without addition, or with 10^9 pfu of phage Clew-1 or phage Ocp-2. The plates were
177 incubated overnight and the next day, the day 2 biofilm mass was quantified using crystal violet. A similar
178 experiment was carried out in 5-mL culture tubes to illustrate the result is shown in Fig. 5A. The averages
179 of 5 biological replicates in the 96-well experiment are shown in Fig. 5B. Treatment of the day one biofilm
180 with phage Clew-1 resulted in a statistically significant decrease in biofilm mass compared to the biomass

181 present at day 1. Phage Ocp-2 infection, on the other hand, did not result in a reduction in biofilm (Fig.
182 5B). Notably, phage Clew-1 was not able to reduce a biofilm formed by *P.* aeruginosa strain PA14, a
183 natural *psl* mutant (Fig. S7).

184 To corroborate this result, we also conducted a converse experiment where we monitored the
185 ability of phage Clew-1 or Ocp-2 to replicate on biofilm bacteria over a two-hour period. Here, biofilms
186 were generated overnight in 5-mL culture tubes, the biofilms were washed with PBS and exposed to 10^5
187 pfu/mL phage Clew-1 or phage Ocp-2 for 2 hours. At the end of the experiment, the culture supernatants
188 were filter sterilized and the phage were titered. Consistent with the reduction in biofilm mass seen in Fig.
189 5B, we found that phage Clew-1, but not Ocp-2, was able to replicate when grown on biofilm bacteria
190 (Fig. 5C).

191

192 **Phage Clew-1 can clear *P. aeruginosa* in a mouse keratitis model**

193 Given the ability of phage Clew-1 to infect *P. aeruginosa* biofilms, we next examined whether
194 Clew-1 could be used to treat a *P. aeruginosa* infection. Corneal infections by *P. aeruginosa* involve
195 formation of a biofilm (8, 40). In fact, a bivalent antibody directed against Psl and the type III secretion
196 needle-tip protein, PcrV, was found to be effective in clearing such corneal infections (8). We therefore
197 examined the ability of Clew-1 to reduce the *P. aeruginosa* bacterial burden in a corneal infection model.
198 Mice were infected with 5*10^4 cfu of wild-type *P. aeruginosa* strain PAO1 and given a topical application
199 of 5*10^9 pfu Clew-1 in 5μL of PBS, or PBS alone, at 3h and 24h post-infection (Fig. 6A). After 48 hours
200 the infection we quantified corneal opacity, a measure that correlates with the infiltration of immune cells
201 (41-43), and GFP fluorescence (produced by the *P. aeruginosa* strain used in the infection) by image
202 analysis. We also assessed the bacterial burden (colony forming units). Mice infected with PAO1
203 developed severe corneal disease manifest as corneal opacification in the region of bacterial growth
204 indicated by GFP fluorescence (Figure S8). Phage Clew-1 treatment was able to significantly reduce the
205 bacterial burden as measured by GFP fluorescence and CFU (Fig. 6C, D). Corneal opacity, however,
206 was not significantly reduced, suggesting that more time would be needed for the inflammation to resolve
207 (Fig. 6B).

208

209 **Summary**

210 We describe the isolation of four phage belonging to the family of Bruynogheviruses that use the
211 *P. aeruginosa* exopolysaccharide Psl as a receptor. Psl is not a capsular polysaccharide, so this
212 distinguishes the Clew phages from phages such as KP32 that infect *Klebsiella pneumoniae*. Moreover,
213 these *Klebsiella* phages use a capsular depolymerase to break down the capsular polysaccharide (44,
214 45). Clew-1, on the other hand, has no such activity (Fig. S9) arguing that the role of Psl in infection is
215 distinct from that seen in capsule-targeting bacteriophage.

216 Phage Clew-1 has the surprising quality that it fails to plaque on wild-type *P. aeruginosa* PAO1,
217 but forms plaques on a *fliF* mutant. We determined that the *fliF* mutation generates a c-di-GMP dependent
218 signal that up-regulates Psl production. Importantly, it increases the fraction of bacteria to which the
219 phage can bind, resulting in efficient lysis in liquid cultures, and plaque formation in top agar. Plaque
220 formation is likely masked in the wild-type bacteria by the fraction of cells that are not phage-susceptible.
221 Notably, certain bruynogheviruses are able to bind to *P. aeruginosa* PAO1, but not plaque (46). We now
222 have an explanation for this observation.

223 The identification of Psl as phage receptor prompted us to examine the ability of phage Clew-1 to
224 infect wild-type *P. aeruginosa* in a biofilm. We found that phage Clew-1, unlike the unrelated Ocp-2 phage,
225 was able to disrupt biofilms formed by wild-type bacteria. Moreover, Clew-1 was able to actively replicate
226 on biofilm bacteria, while phage Ocp-2 could not. Taken together, our data suggests that phage Clew-1
227 has specialized to replicate on *P. aeruginosa* growing in a biofilm. Given the prevalence of bacterial
228 biofilms in nature, this specialization makes sense. Moreover, our observation suggests that we may
229 have underestimated the prevalence of biofilm-tropic bacteriophage since standard isolation techniques
230 using plaque formation of wild-type bacteria would miss phage akin to Clew-1. In fact, another
231 bacteriophage was recently described that requires an intact *psl* operon for replication and can only
232 plaque on PAO1 with elevated c-di-GMP levels (35). This bacteriophage, Knedl, belongs to the family of
233 Igggyvirueses (47), highlighting that more biofilm-tropic bacteriophage wait to be discovered. Our data
234 also suggest that, for *P. aeruginosa*, using a Δ*fliF* Δ*pilA* double mutant will allow us to enrich for biofilm-
235 specific bacteriophage, by excluding dominant type IV pilus-dependent phage and up-regulating biofilm-
236 specific surface structures such as Psl, Pel, and CdrA. Given the importance of biofilms in contributing to

237 the antibiotic resistance of *P. aeruginosa* in infections such as the CF lung, catheters or wound infections,
238 treatment modalities that are targeted towards biofilm bacteria are sorely needed. Indeed, phage Clew-
239 1 shows some promise in this regard, since it was able to control *P.* aeruginosa infection in a mouse
240 model of keratitis, which involves biofilm formation at the site of infection. While many bacteriophages
241 are not able to infect *P. aeruginosa* biofilms, some phage with the ability to target biofilms have been
242 described, including the Bruynoghevirus Delta (18). We present here a way by which phage that target
243 *P. aeruginosa* biofilms can be enriched during isolation.

244 Another interesting aspect of the work described herein is the relationship between the presence
245 of the MS-ring (FliF) and its associated proteins FliE and FliG with c-di-GMP levels. While it has been
246 noted previously that flagellar mutations lead to increases in c-di-GMP levels and increased production
247 of Psl upon surface contact (48), our results differ somewhat in that phage susceptibility was primarily
248 the result of loss of the MS-ring and associated proteins (FliEFG), not, for example, the flagellar filament
249 (FliC). This difference may be due to differences between planktonically grown (as in our study) and
250 surface-attached bacteria. Surface contact leads to up-regulation of c-di-GMP through surface sensing
251 by the wsp chemosensory system (31, 49). Attached bacteria divide asymmetrically, with c-di-GMP levels
252 decreasing in the flagellated daughter cell (33-35, 50). This asymmetry requires the phosphodiesterase
253 Pch, which has been reported to bind to the chemosensory protein CheA (33, 34). A second
254 phosphodiesterase, BifA, is also required for maintaining c-di-GMP homeostasis and developing an
255 asymmetric program of cell division upon attachment to surfaces (35, 36). In our TnSeq experiment we
256 found that insertions in flagellar genes, such as *fliF* and *fliG*, but also insertions in *pch* and *bifA* resulted
257 in Clew-1 sensitivity. Whether the strong Clew-1 sensitivity associated with deletion of *fliF*, *fliE*, or *fliG* in
258 our data, relative to deletions in other flagellar components, relates to a pivotal role of the MS-ring in
259 controlling the activity of Pch and/or BifA is unclear, but worth further investigation. However, our work,
260 along with the work of the Jenal group (35), suggests that phage such as Clew-1 or Knedl could be a
261 useful tool for interrogating c-di-GMP signaling pathways in *P. aeruginosa*.

262 In summary, we have described here the isolation of a group of bacteriophages that target *P.*
263 *aeruginosa* biofilms by using the exopolysaccharide Psl as a receptor. Consistent with the critical role of
264 Psl as part of the *P. aeruginosa* biofilm matrix, we demonstrate that phage Clew-1 can replicate on biofilm

265 bacteria and control *P. aeruginosa* in a mouse model of keratitis. Moreover, we have described a
266 generalizable method that allows for the enrichment of biofilm-tropic bacteriophage, which is important
267 due to their potential utility in combating biofilm infections that are notoriously recalcitrant to antibiotic
268 therapy.
269
270

271 **Methods**

272 *Strain construction and culture conditions*

273 Bacterial strains were grown in LB (10g/L tryptone, 5g/L yeast extract, 5g/L NaCl) at 37°C unless
274 indicated otherwise. Bacterial strains and plasmids used in this study are listed in table S1. Mutations
275 were introduced into the genome of *P. aeruginosa* by allelic exchange. Briefly, flanks defining the mutation
276 were amplified from the *P. aeruginosa* genome and cloned into plasmid pEXG2 by Gibson cloning. The
277 primers used for the amplifications were designed using AmplifX 2.1.1 by Nicolas Jullien (Aix-Marseille
278 Univ, CNRS, INP, Inst Neurophysiopathol, Marseille, France - https://inp.univ-amu.fr/en/amplifx-manage-
279 test-and-design-your-primers-for-pcr) and are noted in table S2. Plasmid pEXG2 harboring the mutation
280 construct was transformed into *E. coli* strain SM10 and mated at 37°C into *P. aeruginosa* by mixing the
281 donor and recipient strains on an LB plate. The mating mixture was then plated on an LB plate with
282 30µg/mL gentamicin and 5µg/mL triclosan and grown overnight at 37°C (selecting against the *E. coli*
283 donor strain). Cointegrates were restruck and subsequently grown in LB lacking salt until the culture was
284 barely turbid. The bacteria were then plated on a sucrose plate (5% sucrose, 10g/L tryptone, 5g/L yeast
285 extract) and incubated overnight at 30°C. Sucrose resistant colonies were tested for gentamicin
286 sensitivity and the presence of the mutation was tested by PCR.

287 Complementing plasmids were generated by amplifying the open reading frame and using Gibson
288 assembly (51) to clone it into pPSV37. The plasmids were then transformed into *P. aeruginosa* by
289 electroporation.

290 For motility assays, individual bacterial colonies were used to inoculate motility agar plates (0.3%
291 agar, LB plates) and incubated at 37°C for ~8h before imaging the plate.

292

293 *CsCl purification of bacteriophage*

294 Bacteriophage were purified by CsCl gradient based on a published protocol (52). Briefly, a 500mL culture
295 of PAO1F Δ*fliF2* was grown in LB to an OD_{600} of ~0.2 and inoculated with phage Clew-1 or Ocp-2 at an
296 MOI of 0.025. After about 4h of culture, the bacteria were pelleted (12,000 x g, 15 min, 4 ºC) and the
297 supernatant was filtered through a 0.2µM filter. The supernatant was treated with DNAse and RNAse
298 (1µg/mL each) overnight at 4°C. The following day, the phage were pelleted by centrifugation (overnight,

299 7,000 x g, 4 ºC), the supernatant discarded and the pellets were resuspended in 1mL of SM buffer (50mM
300 Tris.Cl (pH 7.5), 100mM NaCl, 8mM $MgSO_4$) without BSA each (~2h at 4°C). The concentrated phage
301 prep was then spun at 12,000xg for 10 minutes to pellet remaining cell debris. At this point, 0.75g of
302 CsCl/mL was added to the cleared supernatant and the mixture was spun for 20h at 4°C at 32000 rpm in
303 Beckman Optima MAX-TL ultracentrifuge using an MLS-50 rotor to establish the gradient. The band with
304 the phage was removed with a syringe and 20 gauge needle and transferred to a 3.5kDa cut-off dialysis
305 cassette (Slide-A-Lyzer, Thermo). The phage prep was dialyzed overnight against SM, then 2x for 3h
306 against SM, then overnight against PBS and 1x for 4h against PBS. The phage prep was tested for titer
307 and, in the case of Clew-1, the ability to plaque on a Δ*fliF2* mutant, but not wild-type PAO1F.
308
309 *Negative Stain Electron Microscopy*
310 The negative stain experiment was done as described previously (53). Briefly, a 3 μl phage Clew-
311 1 sample (0.1-0.5 mg/ml) was loaded onto glow-discharge carbon coated grid for 60 s at room
312 temperature and blotted with filter paper. The grid was touched with a water droplet and then blotted with
313 filter paper. This process was repeated twice. The grid was then touched with a drop of 0.75% uranyl
314 formate and blotted with filter paper. A second drop of 0.75% uranyl formate was applied to touch the grid
315 for 30 s, blotted with filter paper and then air dried before data collection. The images were taken by
316 Tecnai T20 (FEI Company) equipped with a Gatan 4K x 4K CCD camera at 80,000 x magnification.
317
318 *Efficiency of plating experiments*
319 To test phage plating efficiency, bacterial strains were back-diluted 1:200 from overnight cultures and
320 grown to early log phase (OD600 ~0.3). At this point, 50μL of culture were mixed with 3mL top agar (10g/L
321 tryptone, 5g/L yeast extract, 5g/L NaCl, 0.6% agar) and plated on an LB agar plate. Once solidified, 10-
322 fold serial dilutions of the phage in SMB buffer (50mM Tris.Cl (pH 7.5), 100mM NaCl, 8mM $MgSO_4$, 0.1%
323 bovine serum albumin). were spotted onto the agar using a multichannel pipette (3μL spots). The spots
324 were allowed to dry and the plates incubated overnight at 37°.
325
326 *Efficiency of Center of Infection (ECOI) experiments*

327 *P. aeruginosa* strains were grown to mid-logarithmic phase in LB supplemented with 5mM MgCl2
328 and 0.1mM MnCl2 (LBMM) concentrated and resuspended at a concentration of 10^9 cfu/mL in LBMM.
329 100µL bacterial suspensions were infected at an MOI of 1 with phage Clew-1 (2µL, 5*10^10 pfu/mL) for
330 5 mins at 37°C, then pelleted (3' 10k RPM), washed 2x with 1mL LB, and resuspended in 100µL LB. The
331 infected cells were serially diluted 10x, then 10µL of diluted, infected bacteria (10^-4 for WT and Δ*fliF2*;
332 10^-1 for Δ*pslC* and Δ*fliF2* Δ*pslC*) were mixed with 50µL of the mid-log PAO1F Δ*fliF2* culture and mixed
333 with 2.5mL top agar, plated on an LB plate and incubated overnight at 37·C. The following day, plaques
334 were counted to enumerate the cell-associated bacteria (54).
335
336 *TnSeq analysis*.
337 Strain PAO1F or PAO1F Δ*fliF* were mutagenized with transposon TnFac (32), a mini-mariner transposon
338 conferring gentamicin resistance. A pool 3*10^6 (PAO1F) or 6*10^6 (PAO1F Δ*fliF*) insertion mutants was
339 grown overnight, then diluted 1:200 in fresh LB and grown to an OD600 of 0.2. At this point the bacteria
340 were infected at an MOI of 10 with phage Clew-1 and incubated for 2h to allow infection and killing of
341 susceptible bacteria. Bacteria from 1mL culture were then pelleted, resuspended in 100µL LB with 5mM
342 EGTA, and plated on a 3 LB plates with 30µg/mL gentamicin. The next day, surviving bacteria that had
343 grown up where pooled and chromosomal DNA from the input and output pools were isolated using the
344 GenElute™ Bacterial Genomic DNA Kit (Millipore-Sigma). Library preparation followed a published
345 protocol (55). Genomic DNA was sheared to ~300bp using a Covaris focused ultrasonicator. The sheared
346 DNA was repaired using the NEBNext End Repair Module (New England Biolabs) and subsequently
347 tailed with a polly-dC tail using Terminal Transferase (New England Biolabs). Tailed chromosomal DNA
348 fragments were amplified in two consecutive steps, using primers Mar1x and olj376 for the first round
349 and Mar2-InSeq paired with a TdT_Index primer for the second round, based on the published protocol
350 (55). The libraries were sequenced using an Illumina MiniSeq system using the transposon-specific
351 primer MarSeq2. Reads with the correct Tn end sequence were mapped and tallied per site and per gene
352 using previously described scripts ((55) and https://github.com/lg9/Tn-seq). The data (hits and # of reads
353 for each gene) are listed for each strain and condition in Table S3.
354

355 *Clew-1 attachment by fluorescence microscopy*

356 Bacteriophage Clew-1 was isolated from 500mL of culture and purified using a CsCl gradient, following
357 a protocol published by the Center for Phage Technology at Texas A&M University. After dialysis overnight
358 dialysis of the phage into SM buffer, the phage was dialyzed 3 more times against PBS (2x for 3h and
359 once overnight). The purified phage was titered by efficiency of plating analysis and labeled with a
360 Dylight594 NHS-ester (Invigtrogen) at a concentration of 0.2mM, overnight in the dark. After labeling, the
361 residual dye was removed by gel filtration using a Performa DTR gel filtration cartridge (EdgeBio) that
362 had been equilibrated with PBS. The labeled phage preparation was titered to ensure that the phage
363 concentration was unchanged and that the phage had not lost infectivity.

364 To assess phage attachment, wild type PAO1F, PAO1F Δ*fliF2*, or PAO1F Δ*fliF2* Δ*pslC* harboring plasmid
365 pP25-GFPo, which directs the constitutive production of GFP, were grown in LB to an OD_{600} of ~0.3-0.4,
366 normalized to an OD_{600} of 03, and 0.5mL of the culture were infected for 10 minutes at 37°C with
367 DyLight594-labeled Clew-1 phage at an MOI of 5. At this point, the infected bacteria were fixed with 1.6%
368 paraformaldehyde [final concentration], incubated in the dark for 10 minutes, then the remaining
369 paraformaldehyde was quenched through the addition of 200μL of 1M glycine (10 minutes at RT). The
370 bacteria were washed 3x with 500μL of SM buffer and resuspended in 30μL SM buffer. 4μL were spotted
371 onto an agarose pad, covered with a coverslip and imaged using a Nikon Eclipse 90i fluorescence
372 microscope. Images were adjusted for contrast and false-colored using the Acorn software package
373 (Flying Meat Software), and cell-associated bacteriophage were counted in ImageJ.

374

375 *Isolation and purification of Psl polysaccharide*

376 Wild-type *P. aerugnoosa* was grown for 18h in M63 minimal medium ($[NH_4]_2SO_4$, 2 g/l; KH_2PO_4, 13.6 g/l;
377 $FeCl_3$, 0.5 mg/l, pH 7) supplemented with 0.5% Casamino acids (BD), 1 mM $MgCl_2$, and 0.2% glucose.
378 Bacterial cells were removed by centrifugation, the supernatant lyophilized, and Psl isolated by affinity
379 chromatography.

380 The affinity column was prepared by resuspending 0.286 g of CNBr activated Sepharose
381 (Purchased from GE Healthcare; cat#17-0430-01) in 1 M HCl (1 mL). It was subsequently filtered and
382 washed with 1 M HCl (60 mL) and coupling buffer (1.5 mL; 0.1 M NaHCO3, 0.5 M NaCl, pH = 9). The

383 activated Sepharose was added to a solution of Cam-003 (56) in coupling buffer (0.5 mL; 10 mg/mL) and
384 was incubated for two hours at room temperature. The solvent was then removed by filtration, and the
385 beads were washed with coupling buffer (3 × 1 mL). After removal of the solvent the sepharose was
386 incubated with blocking buffer (2 mL; 0.1 M Tris, 0.5 M NaCl, pH = 8.5) for 2h at ambient temperature.
387 The beads were washed with wash buffer (4 mL) and coupling buffer (4 mL) for four cycles until the
388 OD280 of the wash was <0.01. The derivatized beads were loaded onto a column and after washing with
389 5 column volumes of PBS-buffer (pH=7.4) the affinity column was ready to use.

390 Crude Psl (100 mg) was dialyzed (Thermo Scientific SnakeSkinTM Dialysis Tubing 3K MWCO)
391 for three days and six exchanges of water and then concentrated to a final volume of 1 mL (10 mg/mL).
392 It was loaded onto the affinity column and washed with PBS-buffer (4 mL) in order to remove all not-
393 retained material. Next, the captured Psl was eluted with glycine buffer (4 mL; 100 mM glycine × HCl,
394 pH=2.7). The glycine fraction was dialyzed (3K MWCO) for three days and six exchanges of water and
395 after lyophilization, pure Psl (80 µg) was obtained.

396 The solution was lyophilized, and the residue was fractionated by gel permeation chromatography
397 on a Bio-Gel P-2 column (90 × 1.5 cm), eluted with 10 mM NH_4HCO_3. The collected fractions contained
398 different size of Psl material: dimer (two repeating units), trimer (three repeating units) and high molecular
399 weight polysaccharide. The high molecular weight polysaccharide fraction was used in our experiments.

400 Matrix-Assisted Laser Desorption/Ionization Time-of-Flight Mass Spectrometry experiments were
401 performed using Bruker ultrafleXtreme (Bruker Daltonics) mass spectrometer. All spectra were recorded
402 in reflector positive-ion mode and the acquisition mass range was 200–6000 Da. Samples were prepared
403 by mixing on the target 0.5 µL sample solutions with 0.5 µL aqueous 10% 2,5-dihydroxybenzoic acid as
404 matrix solution.

405

406 *Precipitation of Clew-1 from culture supernatants and using purified Psl*

407 For experiments in which binding of Clew-1 to Psl in culture supernatants was tested, PAO1F
408 Δ*fliF2* or PAO1F Δ*fliF2* Δ*pslC* were grown to mid-logarithmic phase, then the bacteria were pelleted and
409 the supernatants filter sterilized using a 0.2µM filter. Culture supernatants were mixed with 1µL of a rabbit,
410 anti-Psl antibody (37) as well as 10^7 pfu of phage Clew-1. The mixture was incubated on ice for 1h, then

411 10μL of magnetic protein A beads (BioRad), washed 2x with SMB + 0.05% Triton X-100 (SMBT) were
412 added to the mixture and incubated for an additional 30 minutes on ice. The magnetic beads were
413 collected, washed 3x with SMBT and resuspended in 100μl of SMBT. Presence of Clew-1 in input and
414 output samples was determined by quantitative PCR using primers designed to amplify the tail fiber gene,
415 gp12.

416 Experiments using partially purified, cell-associated Psl were carried out in SM buffer. 100μL of
417 SM-buffer were mixed with 10^7 pfu of phage Clew-1, as well as 1μg of a partially purified, deproteinated
418 fraction of cell-associated Psl (57) and incubated for 1h on ice. All subsequent steps were the same as
419 for the culture supernatants, above. Samples were resuspended in 100μL SMBT before quantifying Clew-
420 1 levels.

421 Experiments using affinity purified, biotinylated Psl were carried out in SM. Here too, 10^7 pfu
422 Clew-1 were incubated with 1μg of affinity purified, biotinylated Psl. The samples were either incubated
423 with streptavidin-coated Dynabeads (M280, Invitrogen) to precipitate the biotinylated Psl (or with
424 magnetic protein A beads as a specificity control). Otherwise, the experiments were carried out as for the
425 partially purified, cell-associated Psl fraction, above.

426

427 *Static biofilm experiments*

428 Static biofilm experiments were carried out based on a published protocol (58). *P. aeruginosa* PAO1F
429 was grown to mid-logarithmic phase in LB and then diluted to an OD600 of 0.05 and used to inoculate
430 either 5mL polystyrene tubes (1mL) or 6 wells in a polystyrene 96-well plate (150μL). The cultures were
431 incubated overnight at 37°C in a humidified incubator with a 5% CO2 atmosphere. The following day, 1
432 set of biofilm samples was washed three times with PBS, for 20 minutes fixed with 95% ethanol, and
433 subsequently air dried after removing the ethanol. The remaining biofilm samples were washed 2x with
434 PBS and reconstituted with pre-warmed LB (1.2mL in 5mL tube biofilms, 200μL. in 96-well plates), or LB
435 harboring either 10^9 pfu of phage Clew-1 or phage Ocp-2. The biofilm samples were again incubated
436 overnight at 37°C in a humidified incubator with a 5% CO2 atmosphere, and subsequently washed and
437 fixed as the control samples, above. The fixed and dried biofilms were stained with a 0.1% solution of
438 crystal violet in water for 30 minutes, the staining solution was removed, and the biofilms were washed

439 2x with mili-Q water and rinsed twice with deionized water before drying the stained biofilm samples. The
440 stained biofilms in the 5mL tubes were photographed against a white background. The stained biofilms
441 in the 96-well plates were incubated for 20 minutes in 200µL 30% acetic acid to solubilize the crystal
442 violet stain, which was subsequently quantified by spectrophotometry (absorbance at 590nm).
443
444 *Mouse keratitis model*
445 C57BL/6 mice were purchased from Jackson Laboratories. The mice were housed in pathogen free
446 conditions in microisolator cages and were treated according to institutional guidelines following approval
447 by the University of California IACUC.
448 Overnight cultures of P. aeruginosa PAO1F/pP25-GFPo were grown to log phase (OD_{600} of 0.2) in LB
449 broth, then washed and resuspended in PBS at $2.5x10^7$ bacteria/ml. 7-12 weeks old C57BL/6 mice were
450 anesthetized with ketamine/xylazine solution, the corneal epithelium was abraded with three parallel
451 scratches using a sterile 26-gauge needle, and 2 µL of a suspension of bacteria were added topically
452 (approximately $5x10^4$ cfu per eye). At 3h and 24h, the mice were anesthetized and treated with 2*10^9
453 pfu CsCl purified phage Clew-1 in PBS, or PBS alone. At 48h the mice were euthanized, and corneas
454 were imaged by brightfield microscopy to detect opacification, or by fluorescence microscopy to detect
455 GFP-expressing bacteria. Fluorescent intensity images were quantified using Image J software (NIH).
456 To determine the bacterial load, whole eyes were homogenized in PBS using a TissueLyser II (Qiagen,
457 30 Hz for 3 minutes), and homogenates were serially diluted plated on LB agar plates for quantification
458 of colony forming units (CFU) by manual counting. CFU were also determined at 2 h to confirm the
459 inoculum.
460
461 *Growth curves*
462 Strains PAO1F, PAO1F Δ*fliF2*, PAO1F Δ*pslC*, and PAO1F Δ*fliF2* Δ*pslC* were grown to mid-logarithmic
463 phase in LB, then diluted to a concentration of 10^8 cfu/mL. For growth curve measurements (OD600),
464 3 technical replicates were set up in a 96-well plate for each strain/condition. 100µL of culture were mixed
465 with 10µL PBS or 10µL with 10^8 pfu Clew-1 and incubated at 37°C in an Agilent Cytation 5 Imaging

466 Plate Reader with a heated chamber and orbital rotation between OD600 measurements. OD600
467 readings were taken every 5 minutes.
468
469 *Culture Supernatant Psl blot*
470 Strains PAO1F Δ*fliF2* and PAO1F Δ*fliF2* Δ*pslC* were grown to mid-logarithmic phase (OD600 ~0.5), the
471 bacteria pelleted by centrifugation and the culture supernatant was sterilized using a 0.22μM syringe
472 filter. 0.5mL supernatant samples were incubated for 1h at 37°C with or without 10^7 pfu Clew-1 and
473 subsequently diluted three times at a 1:3 ratio. 2μL of the undiluted culture supernatants and of each
474 dilution were spotted onto a nitrocellulose filter and allowed to air-dry. The filter was then blocked with
475 5% non-fat milk in TBS-T (20mM Tris.Cl, 150mM NaCl, 0.1% Tween-20) for 30 minutes, washed 2x with
476 TBS-T and incubated with the primary anti-Psl antibody (diluted 1:3000) in TBS-T overnight at 4°C. The
477 following day, the blot was washed 3x with TBS-T, then incubated with secondary antibody (horse-radish
478 peroxidase conjugated goat anti-rabbit antibody, Sigma) diluted 1:10000 in TBS-T for ~3h at room
479 temperature. The blot was then washed 3x with TBS-T and developed using the Advansta WesternBright
480 Sirius HRP substrate and imaged on a GE ImageQuant LAS4000 imager.
481
482 *Analysis of Evolutionary Relatedness*
483 The evolutionary relationship between Clew bacteriophage and other Bruynogheviruses was carried out
484 using the Maximum Likelihood method and JTT matrix-based model (59). The tree with the highest log
485 likelihood is shown. Initial tree(s) for the heuristic search were obtained automatically by applying
486 Neighbor-Join and BioNJ algorithms to a matrix of pairwise distances estimated using the JTT model,
487 and then selecting the topology with superior log likelihood value. The tree is drawn to scale, with branch
488 lengths measured in the number of substitutions per site. This analysis involved 12 amino acid
489 sequences. There was a total of 485 positions in the final dataset. Evolutionary analyses were conducted
490 in MEGA11(60, 61). The genome comparison between Luz24 and the Clew phages was visualized using
491 EasyFig (62).
492
493

494 **Acknowledgements**

495 This work was made possible through an award by the Hypothesis fund. The authors would like to thank
496 the Northeast Ohio Regional Sewer District, and in particular Scott Broski and Leslie Vankuren, for
497 providing the wastewater samples from which the bacteriophage described in this study were isolated.
498 We wish to acknowledge Sabrina Lamont and Tony DiCesare (Wozniak lab) who provided Psl
499 preparations and αPsl rabbit polyclonal antibody for the studies described. The authors would like to
500 thank Dr. George Dubyak for the use of his spectrophotometer/plate reader. We would like to thank Dr.
501 Joseph Mougous for providing us with unpublished *pslC* and *pslD* complementation plasmids. We would
502 also like to thank Dr. Mougous and Dr. Simon Dove for their support and for critical reading of the
503 manuscript, and Dr. Matthew Parsek for his enthusiasm for the project and helpful discussions. This
504 manuscript was supported by NIH grant R01AI169865 (to D.J.W.), grant R01EY14362 (to E.P.), and grant
505 R01 AI145069 (to E.W.Y). The Psl-specific CAM003 antibody was obtained by G.-J.B. from AstraZeneca
506 (Dr. Antonio DiGiandomenico).

507

508 **Figure Legends**

509 **Fig. 1 c-di-GMP levels control infection of *P. aeruginosa* by bacteriophage Clew-1.** A) Efficiency
510 of plating experiment in which 3μL of a 10x dilution series of bacteriophage Ocp-2 or Clew-1 were
511 spotted on wild-type PAO1F, or PAO1F Δ*fliF2*. The adjacent graph shows the compiled results from 11
512 experiments. B) Maximum likelihood phylogenetic tree of Clew-1 relative to other Bruynogheviruses
513 (including the type phage, LUZ24) and phage Bjorn as an outgroup. Branch lengths are measured in
514 number of substitutions per site in the terminase large subunit. C) transmission electron micrograph of
515 the Clew-1 phage. D) Efficiency of plating experiment as in (A) assaying the effect of expressing the
516 phosphodiesterase PA2133 from a plasmid. E) Efficiency of plating experiment assaying the effect of
517 deleting *wspF* on Clew-1 resistance. (* $p<0.05$, **** $p<0.0001$ by Student's T-test (A, E) or 1-way
518 ANOVA with Šídák's multiple comparisons test (D))

519

520 **Fig. 2 Bacteriophage Clew-1 uses Psl as a receptor to infect *P. aeruginosa*.** A) TnSeq experiment
521 in which a pool of mariner transposon mutants of strain PAO1F were infected with phage Clew-1 for 2h.
522 The number of insertions in the output pool were plotted against the ratio of the output and input pool.
523 B) Similar TnSeq analysis as in A) but using PAO1F Δ*fliF2*. C) Efficiency of plating analysis on Δ*fliF2*
524 Δ*pslC* and Δ*fliF2* Δ*pslD,* Psl biosynthesis mutants, either harboring an empty vector or a complementing
525 plasmid (n=6). Clew-1 values were compared by 1-way ANOVA with Šídák's multiple comparisons test
526 (** $p<0.01$, n.s. .. not significant).

527

528 **Fig. 3. The Δ*fliF2* mutation changes the fraction of cells that phage Clew-1 binds to**. A) Efficiency
529 of center of infection analysis. The indicated strain was infected for 5 minutes at an MOI of 0.01, the
530 bacteria were pelleted, washed 3x with PBS, then diluted and mixed with an excess of the Δ*fliF2* mutant
531 strain, top agar and plated on an LB agar plate. The number of plaques was used to calculate the
532 number of phage that attached and productively infected the initial strain. B) Phage Clew-1 was labeled
533 with DyLight594 fluorophores, bound to the indicated wild-type or mutant bacteria (15 minutes in LB),
534 washed and fixed with paraformaldehyde. Phage attached to bacteria were imaged by fluorescence
535 microscopy and attachment was quantified over 5 biological replicates, shown in C). Attachment was

536 compared by 1-way ANOVA with Šídák's multiple comparisons test. * p< 0.05, *** p<0.001 ,****
537 p<0.0001.
538
539 **Fig. 4. Phage Clew-1 binds to Psl**. A) Sterile filtered mid-log culture supernatants of PAO1F Δ*fliF2* or
540 PAO1F Δ*fliF2* Δ*pslC* were incubated with phage Clew-1, as well as magnetic protein-A beads and,
541 where indicated, a rabbit, anti-Psl antiserum. Beads were collected, washed 3x, and phage in the input
542 and output samples were quantified by qPCR (7 independent replicates.) B) Phage Clew-1 was
543 incubated for 1h in SM buffer with affinity purified, biotinylated Psl (biotin-Psl) and magnetic protein A
544 beads, or magnetic streptavidin beads (SA), where indicated. Beads were collected and washed 3x,
545 and phage in the input and output samples were quantified by qPCR (3 independent replicates).
546 Statistical significance was determined by ANOVA with Sidák post-hoc test (**** p<0.0001).
547
548 **Fig. 5. Phage Clew-1 can infect *P. aeruginosa* in biofilms**. A) Biofilms of wild type *P.* aeruginosa
549 PAO1F were established overnight in 5mL culture tubes (1mL culture), the tubes were washed with
550 PBS and 1.2mL LB, LB with 10^10 pfu phage Clew-1, or LB-with 10^10 pfu phage Ocp-2 were added
551 back to each tube (1 was fixed with EtOH to represent the 1-day old biofilm). The following day all
552 biofilms were washed with PBS and stained with crystal violet. B) PAO1F biofilms were established
553 overnight in a 96-well plate (150μL of culture, 6 technical replicates/condition), washed and incubated
554 overnight with 200μL of LB or LB with 10^9 pfu bacteriophage Clew-1 or Ocp-2. The biofilms were then
555 washed, fixed, and stained with crystal violet, which was then solubilized with 30% acetic acid and
556 quantified spectrophotometrically at 590 nm. The day 1 controls were set to 100% (5 biological
557 replicates). C) Growth of phage Clew-1 or Ocp-2 was assayed by establishing a static biofilm in 5 mL
558 culture tubes overnight (1mL culture volume). The biofilms were washed with PBS, then 1mL of LB with
559 10^5 pfu/mL of phage Clew-1 or Ocp-2 were added back. Biofilms were incubated at 37°C for 2h 15
560 minutes, the culture supernatants were filter sterilized and input and output phage concentrations were
561 tittered (6 biological replicates). Statistical significance was determined by ANOVA with Šídák's multiple
562 comparisons test test (** p<0.01, *** p<0.001).
563

564 **Fig. 6. Phage Clew-1 reduces the bacterial burden in a mouse cornea model of infection**. A) Mice
565 corneas were scratched and infected with 5*10^4 cfu strain PAO1F/pP25-GFPo, which produces GFP
566 constitutively. Infected corneas were treated with 2*10^9 pfu phage Clew-1 or a PBS control at 3h and
567 24h post infection. B) At 48h post infection, the corneas were imaged by confocal microscopy to
568 estimate the opacity (driven largely by the infiltration of neutrophils) and C) GFP fluorescence
569 (produced by infecting *P. aeruginosa*). D) Eyes were also homogenized and plated for CFU to
570 determine the total bacterial burden at the end of the experiment. Significance was determined by
571 Mann-Whitney test (** $p<0.01$, n.s. not significant).
572

573 **References**

574 1. Wilton M, Charron-Mazenod L, Moore R, Lewenza S. Extracellular DNA Acidifies Biofilms and
575 Induces Aminoglycoside Resistance in Pseudomonas aeruginosa. Antimicrob Agents Chemother.
576 2016;60(1):544-53.
577 2. Chiang WC, Nilsson M, Jensen PO, Hoiby N, Nielsen TE, Givskov M, et al. Extracellular DNA
578 shields against aminoglycosides in Pseudomonas aeruginosa biofilms. Antimicrob Agents Chemother.
579 2013;57(5):2352-61.
580 3. Ciofu O, Moser C, Jensen PO, Hoiby N. Tolerance and resistance of microbial biofilms. Nat Rev
581 Microbiol. 2022;20(10):621-35.
582 4. Lewis K. Multidrug tolerance of biofilms and persister cells. Curr Top Microbiol Immunol.
583 2008;322:107-31.
584 5. Hoiby N, Ciofu O, Bjarnsholt T. Pseudomonas aeruginosa biofilms in cystic fibrosis. Future
585 Microbiol. 2010;5(11):1663-74.
586 6. Mulcahy LR, Burns JL, Lory S, Lewis K. Emergence of Pseudomonas aeruginosa strains
587 producing high levels of persister cells in patients with cystic fibrosis. J Bacteriol. 2010;192(23):6191-9.
588 7. Ledizet M, Murray TS, Puttagunta S, Slade MD, Quagliarello VJ, Kazmierczak BI. The ability of
589 virulence factor expression by Pseudomonas aeruginosa to predict clinical disease in hospitalized
590 patients. PLoS One. 2012;7(11):e49578.
591 8. Thanabalasuriar A, Scott BNV, Peiseler M, Willson ME, Zeng Z, Warrener P, et al. Neutrophil
592 Extracellular Traps Confine Pseudomonas aeruginosa Ocular Biofilms and Restrict Brain Invasion. Cell
593 Host Microbe. 2019;25(4):526-36 e4.
594 9. Behlau I, Gilmore MS. Microbial biofilms in ophthalmology and infectious disease. Arch
595 Ophthalmol. 2008;126(11):1572-81.
596 10. Okurowska K, Monk PN, Karunakaran E. Increased tolerance to commonly used antibiotics in a
597 Pseudomonas aeruginosa ex vivo porcine keratitis model. Microbiology (Reading). 2024;170(5).
598 11. Hamed K, Debonnett L. Tobramycin inhalation powder for the treatment of pulmonary
599 Pseudomonas aeruginosa infection in patients with cystic fibrosis: a review based on clinical evidence.
600 Ther Adv Respir Dis. 2017;11(5):193-209.
601 12. D'Agata EM. Rapidly rising prevalence of nosocomial multidrug-resistant, Gram-negative bacilli:
602 a 9-year surveillance study. Infect Control Hosp Epidemiol. 2004;25(10):842-6.
603 13. Rice LB. Federal funding for the study of antimicrobial resistance in nosocomial pathogens: no
604 ESKAPE. J Infect Dis. 2008;197(8):1079-81.
605 14. Qin S, Xiao W, Zhou C, Pu Q, Deng X, Lan L, et al. Pseudomonas aeruginosa: pathogenesis,
606 virulence factors, antibiotic resistance, interaction with host, technology advances and emerging
607 therapeutics. Signal Transduct Target Ther. 2022;7(1):199.
608 15. Yin C, Alam MZ, Fallon JT, Huang W. Advances in Development of Novel Therapeutic Strategies
609 against Multi-Drug Resistant Pseudomonas aeruginosa. Antibiotics. 2024;13(2):119.
610 16. Luthe T, Kever L, Thormann K, Frunzke J. Bacterial multicellular behavior in antiviral defense.
611 Curr Opin Microbiol. 2023;74:102314.
612 17. Manohar P, Loh B, Turner D, Tamizhselvi R, Mathankumar M, Elangovan N, et al. In vitro and in
613 vivo evaluation of the biofilm-degrading Pseudomonas phage Motto, as a candidate for phage therapy.
614 Frontiers in microbiology. 2024;15:1344962.
615 18. Knezevic P, Petrovic Fabijan A, Gavric D, Pejic J, Doffkay Z, Rakhely G. Phages from Genus
616 Bruynoghevirus and Phage Therapy: Pseudomonas Phage Delta Case. Viruses. 2021;13(10).
617 19. Ma LZ, Wang D, Liu Y, Zhang Z, Wozniak DJ. Regulation of Biofilm Exopolysaccharide
618 Biosynthesis and Degradation in Pseudomonas aeruginosa. Annu Rev Microbiol. 2022;76:413-33.
619 20. Ma L, Conover M, Lu H, Parsek MR, Bayles K, Wozniak DJ. Assembly and development of the
620 Pseudomonas aeruginosa biofilm matrix. PLoS Pathog. 2009;5(3):e1000354.
621 21. Byrd MS, Pang B, Mishra M, Swords WE, Wozniak DJ, Pier G. The Pseudomonas aeruginosa
622 Exopolysaccharide Psl Facilitates Surface Adherence and NF-κB Activation in A549 Cells. mBio.
623 2010;1(3).
624 22. Colvin KM, Irie Y, Tart CS, Urbano R, Whitney JC, Ryder C, et al. The Pel and Psl polysaccharides
625 provide Pseudomonas aeruginosa structural redundancy within the biofilm matrix. Environ Microbiol.
626 2012;14(8):1913-28.

627 23. Zhao K, Tseng BS, Beckerman B, Jin F, Gibiansky ML, Harrison JJ, et al. Psl trails guide
628 exploration and microcolony formation in Pseudomonas aeruginosa biofilms. Nature.
629 2013;497(7449):388-91.
630 24. Mishra M, Byrd MS, Sergeant S, Azad AK, Parsek MR, McPhail L, et al. Pseudomonas aeruginosa
631 Psl polysaccharide reduces neutrophil phagocytosis and the oxidative response by limiting complement-
632 mediated opsonization. Cell Microbiol. 2012;14(1):95-106.
633 25. Lefkowitz EJ, Dempsey DM, Hendrickson RC, Orton RJ, Siddell SG, Smith DB. Virus taxonomy:
634 the database of the International Committee on Taxonomy of Viruses (ICTV). Nucleic Acids Res.
635 2018;46(D1):D708-D17.
636 26. Minamino T, Kawamoto A, Kinoshita M, Namba K. Molecular Organization and Assembly of the
637 Export Apparatus of Flagellar Type III Secretion Systems. Bacterial Type III Protein Secretion Systems.
638 Current Topics in Microbiology and Immunology2019. p. 91-107.
639 27. Erhardt M, Wheatley P, Kim EA, Hirano T, Zhang Y, Sarkar MK, et al. Mechanism of type-III protein
640 secretion: Regulation of FlhA conformation by a functionally critical charged-residue cluster. Mol
641 Microbiol. 2017;104(2):234-49.
642 28. Arora SK, Ritchings BW, Almira EC, Lory S, Ramphal R. A transcriptional activator, FleQ,
643 regulates mucin adhesion and flagellar gene expression in Pseudomonas aeruginosa in a cascade
644 manner. J Bacteriol. 1997;179(17):5574-81.
645 29. Oladosu VI, Park S, Sauer K. Flip the switch: the role of FleQ in modulating the transition between
646 the free-living and sessile mode of growth in Pseudomonas aeruginosa. J Bacteriol.
647 2024;206(3):e0036523.
648 30. Dasgupta N, Wolfgang MC, Goodman AL, Arora SK, Jyot J, Lory S, et al. A four-tiered
649 transcriptional regulatory circuit controls flagellar biogenesis in Pseudomonas aeruginosa. Molecular
650 Microbiology. 2003;50(3):809-24.
651 31. Hickman JW, Tifrea DF, Harwood CS. A chemosensory system that regulates biofilm formation
652 through modulation of cyclic diguanylate levels. Proc Natl Acad Sci U S A. 2005;102(40):14422-7.
653 32. Wong SM, Mekalanos JJ. Genetic footprinting with mariner-based transposition in Pseudomonas
654 aeruginosa. Proc Natl Acad Sci U S A. 2000;97(18):10191-6.
655 33. Kulasekara BR, Kamischke C, Kulasekara HD, Christen M, Wiggins PA, Miller SI. c-di-GMP
656 heterogeneity is generated by the chemotaxis machinery to regulate flagellar motility. eLife. 2013;2.
657 34. Laventie B-J, Sangermani M, Estermann F, Manfredi P, Planes R, Hug I, et al. A Surface-Induced
658 Asymmetric Program Promotes Tissue Colonization by Pseudomonas aeruginosa. Cell Host & Microbe.
659 2019;25(1):140-52.e6.
660 35. Manner C, Dias Teixeira R, Saha D, Kaczmarczyk A, Zemp R, Wyss F, et al. A genetic switch
661 controls Pseudomonas aeruginosa surface colonization. Nat Microbiol. 2023;8(8):1520-33.
662 36. Kuchma SL, Brothers KM, Merritt JH, Liberati NT, Ausubel FM, O'Toole GA. BifA, a cyclic-Di-GMP
663 phosphodiesterase, inversely regulates biofilm formation and swarming motility by Pseudomonas
664 aeruginosa PA14. J Bacteriol. 2007;189(22):8165-78.
665 37. Byrd MS, Sadovskaya I, Vinogradov E, Lu H, Sprinkle AB, Richardson SH, et al. Genetic and
666 biochemical analyses of the Pseudomonas aeruginosa Psl exopolysaccharide reveal overlapping roles
667 for polysaccharide synthesis enzymes in Psl and LPS production. Molecular Microbiology.
668 2009;73(4):622-38.
669 38. Wu H, Wang D, Tang M, Ma LZ. The advance of assembly of exopolysaccharide Psl biosynthesis
670 machinery in Pseudomonas aeruginosa. Microbiologyopen. 2019;8(10):e857.
671 39. Tabor DE, Oganesyan V, Keller AE, Yu L, McLaughlin RE, Song E, et al. Pseudomonas
672 aeruginosa PcrV and Psl, the Molecular Targets of Bispecific Antibody MEDI3902, Are Conserved Among
673 Diverse Global Clinical Isolates. J Infect Dis. 2018;218(12):1983-94.
674 40. Zegans ME, DiGiandomenico A, Ray K, Naimie A, Keller AE, Stover CK, et al. Association of
675 Biofilm Formation, Psl Exopolysaccharide Expression, and Clinical Outcomes in Pseudomonas
676 aeruginosa Keratitis: Analysis of Isolates in the Steroids for Corneal Ulcers Trial. JAMA ophthalmology.
677 2016;134(4):383-9.
678 41. Sun Y, Karmakar M, Roy S, Ramadan RT, Williams SR, Howell S, et al. TLR4 and TLR5 on corneal
679 macrophages regulate Pseudomonas aeruginosa keratitis by signaling through MyD88-dependent and -
680 independent pathways. J Immunol. 2010;185(7):4272-83.

42. Hazlett LD, Zucker M, Berk RS. Distribution and kinetics of the inflammatory cell response to ocular challenge with Pseudomonas aeruginosa in susceptible versus resistant mice. Ophthalmic Res. 1992;24(1):32-9.
43. Lee EJ, Cowell BA, Evans DJ, Fleiszig SM. Contribution of ExsA-regulated factors to corneal infection by cytotoxic and invasive Pseudomonas aeruginosa in a murine scarification model. Invest Ophthalmol Vis Sci. 2003;44(9):3892-8.
44. Squeglia F, Maciejewska B, Łątka A, Ruggiero A, Briers Y, Drulis-Kawa Z, et al. Structural and Functional Studies of a Klebsiella Phage Capsule Depolymerase Tailspike: Mechanistic Insights into Capsular Degradation. Structure. 2020;28(6):613-24.e4.
45. Dunstan RA, Bamert RS, Belousoff MJ, Short FL, Barlow CK, Pickard DJ, et al. Mechanistic Insights into the Capsule-Targeting Depolymerase from a Klebsiella pneumoniae Bacteriophage. Microbiology Spectrum. 2021;9(1).
46. Costa AR, van den Berg DF, Esser JQ, Muralidharan A, van den Bossche H, Bonilla BE, et al. Accumulation of defense systems in phage-resistant strains of Pseudomonas aeruginosa. Sci Adv. 2024;10(8):eadj0341.
47. Maffei E, Manner C, Jenal U, Harms A. Complete genome sequence of Pseudomonas aeruginosa phage Knedl. Microbiol Resour Announc. 2024;13(4):e0117423.
48. Garsin DA, Harrison JJ, Almblad H, Irie Y, Wolter DJ, Eggleston HC, et al. Elevated exopolysaccharide levels in Pseudomonas aeruginosa flagellar mutants have implications for biofilm growth and chronic infections. PLOS Genetics. 2020;16(6).
49. Armbruster CR, Lee CK, Parker-Gilham J, de Anda J, Xia A, Zhao K, et al. Heterogeneity in surface sensing suggests a division of labor in Pseudomonas aeruginosa populations. eLife. 2019;8.
50. Christen M, Kulasekara HD, Christen B, Kulasekara BR, Hoffman LR, Miller SI. Asymmetrical distribution of the second messenger c-di-GMP upon bacterial cell division. Science. 2010;328(5983):1295-7.
51. Gibson DG, Young L, Chuang RY, Venter JC, Hutchison CA, 3rd, Smith HO. Enzymatic assembly of DNA molecules up to several hundred kilobases. Nat Methods. 2009;6(5):343-5.
52. Piya D, Vara L, Russell WK, Young R, Gill JJ. The multicomponent antirestriction system of phage P1 is linked to capsid morphogenesis. Mol Microbiol. 2017;105(3):399-412.
53. Booth DS, Avila-Sakar A, Cheng Y. Visualizing proteins and macromolecular complexes by negative stain EM: from grid preparation to image acquisition. J Vis Exp. 2011(58).
54. Hyman P, Abedon ST. Bacteriophage host range and bacterial resistance. Adv Appl Microbiol. 2010;70:217-48.
55. Gallagher LA. Methods for Tn-Seq Analysis in Acinetobacter baumannii. Methods Mol Biol. 2019;1946:115-34.
56. DiGiandomenico A, Warrener P, Hamilton M, Guillard S, Ravn P, Minter R, et al. Identification of broadly protective human antibodies to Pseudomonas aeruginosa exopolysaccharide Psl by phenotypic screening. J Exp Med. 2012;209(7):1273-87.
57. Chiba A, Sugimoto S, Sato F, Hori S, Mizunoe Y. A refined technique for extraction of extracellular matrices from bacterial biofilms and its applicability. Microb Biotechnol. 2015;8(3):392-403.
58. O'Toole GA. Microtiter dish biofilm formation assay. J Vis Exp. 2011(47).
59. Jones DT, Taylor WR, Thornton JM. The rapid generation of mutation data matrices from protein sequences. Comput Appl Biosci. 1992;8(3):275-82.
60. Stecher G, Tamura K, Kumar S. Molecular Evolutionary Genetics Analysis (MEGA) for macOS. Mol Biol Evol. 2020;37(4):1237-9.
61. Tamura K, Stecher G, Kumar S. MEGA11: Molecular Evolutionary Genetics Analysis Version 11. Mol Biol Evol. 2021;38(7):3022-7.
62. Sullivan MJ, Petty NK, Beatson SA. Easyfig: a genome comparison visualizer. Bioinformatics. 2011;27(7):1009-10.

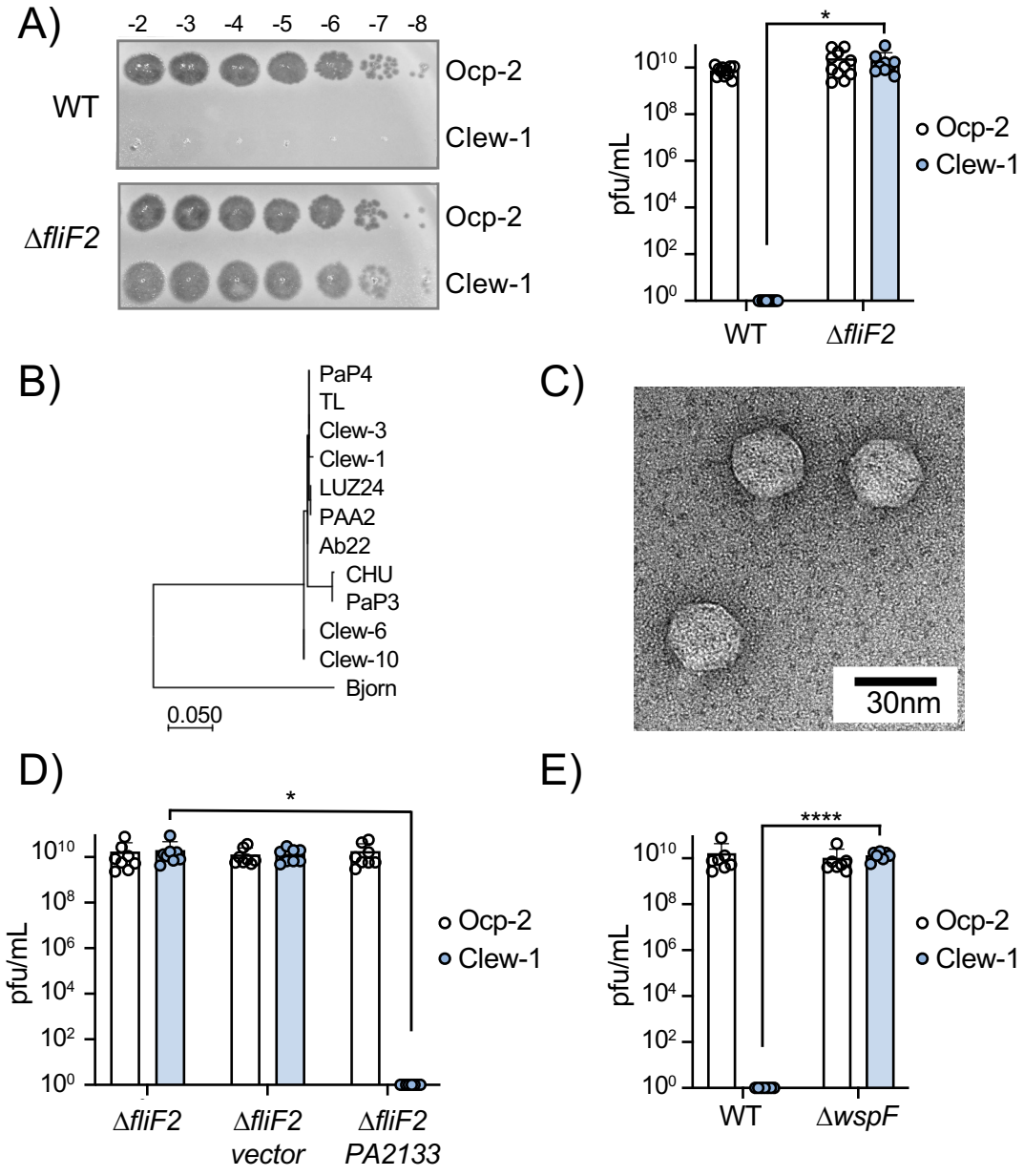

Fig. 1 c-di-GMP levels control infection of *P. aeruginosa* by bacteriophage Clew-1. A) Efficiency of plating experiment in which 3μL of a 10x dilution series of bacteriophage Ocp-2 or Clew-1 were spotted on wild-type PAO1F, or PAO1F Δ*fliF2*. The adjacent graph shows the compiled results from 11 experiments. B) Maximum likelihood phylogenetic tree of Clew-1 relative to other Bruynogheviruses (including the type phage, LUZ24) and phage Bjorn as an outgroup. Branch lengths are measured in number of substitutions per site in the terminase large subunit. C) transmission electron micrograph of the Clew-1 phage. D) Efficiency of plating experiment as in (A) assaying the effect of expressing the phosphodiesterase PA2133 from a plasmid. E) Efficiency of plating experiment assaying the effect of deleting *wspF* on Clew-1 resistance. (* $p<0.05$, **** $p<0.0001$ by Student's T-test (A, E) or 1-way ANOVA with Šídák's multiple comparisons test (D))

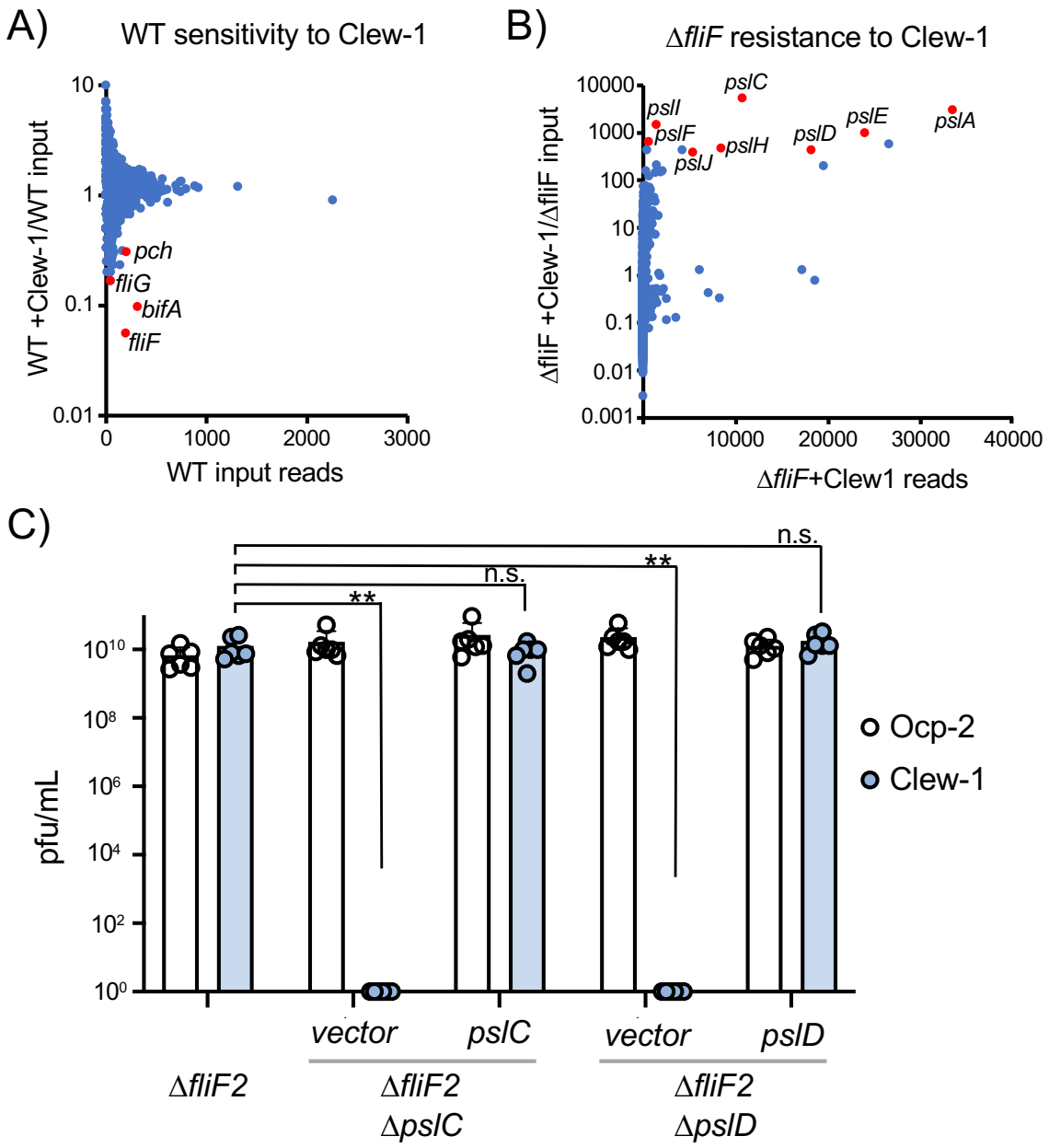

Fig. 2 Bacteriophage Clew-1 uses Psl as a receptor to infect *P. aeruginosa*. A) TnSeq experiment in which a pool of mariner transposon mutants of strain PAO1F were infected with phage Clew-1 for 2h. The number of insertions in the output pool were plotted against the ratio of the output and input pool. B) Similar TnSeq analysis as in A) but using PAO1F Δ*fliF2*. C) Efficiency of plating analysis on Δ*fliF2* Δ*pslC* and Δ*fliF2* Δ*pslD,* Psl biosynthesis mutants, either harboring an empty vector or a complementing plasmid (n=6). Clew-1 values were compared by 1-way ANOVA with Šídák's multiple comparisons test (** $p<0.01$, n.s. .. not significant).

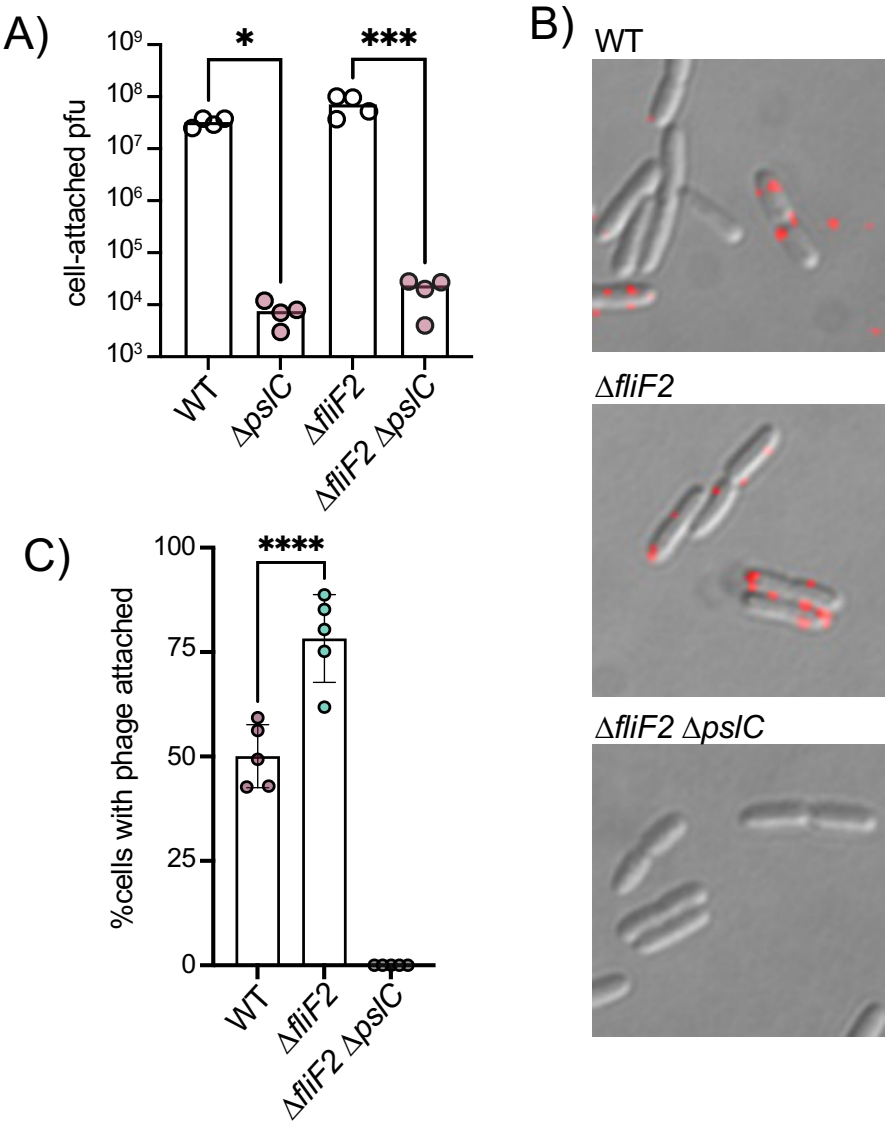

Fig. 3. The Δ*fliF2* mutation changes the fraction of cells that phage Clew-1 binds to. A) Efficiency of center of infection analysis. The indicated strain was infected for 5 minutes at an MOI of 0.01, the bacteria were pelleted, washed 3x with PBS, then diluted and mixed with an excess of the Δ*fliF2* mutant strain, top agar and plated on an LB agar plate. The number of plaques was used to calculate the number of phage that attached and productively infected the initial strain. B) Phage Clew-1 was labeled with DyLight594 fluorophores, bound to the indicated wild-type or mutant bacteria (15 minutes in LB), washed and fixed with paraformaldehyde. Phage attached to bacteria were imaged by fluorescence microscopy and attachment was quantified over 5 biological replicates, shown in C). Attachment was compared by 1-way ANOVA with Šídák's multiple comparisons test. * $p < 0.05$, *** $p<0.001$,**** $p<0.0001$.

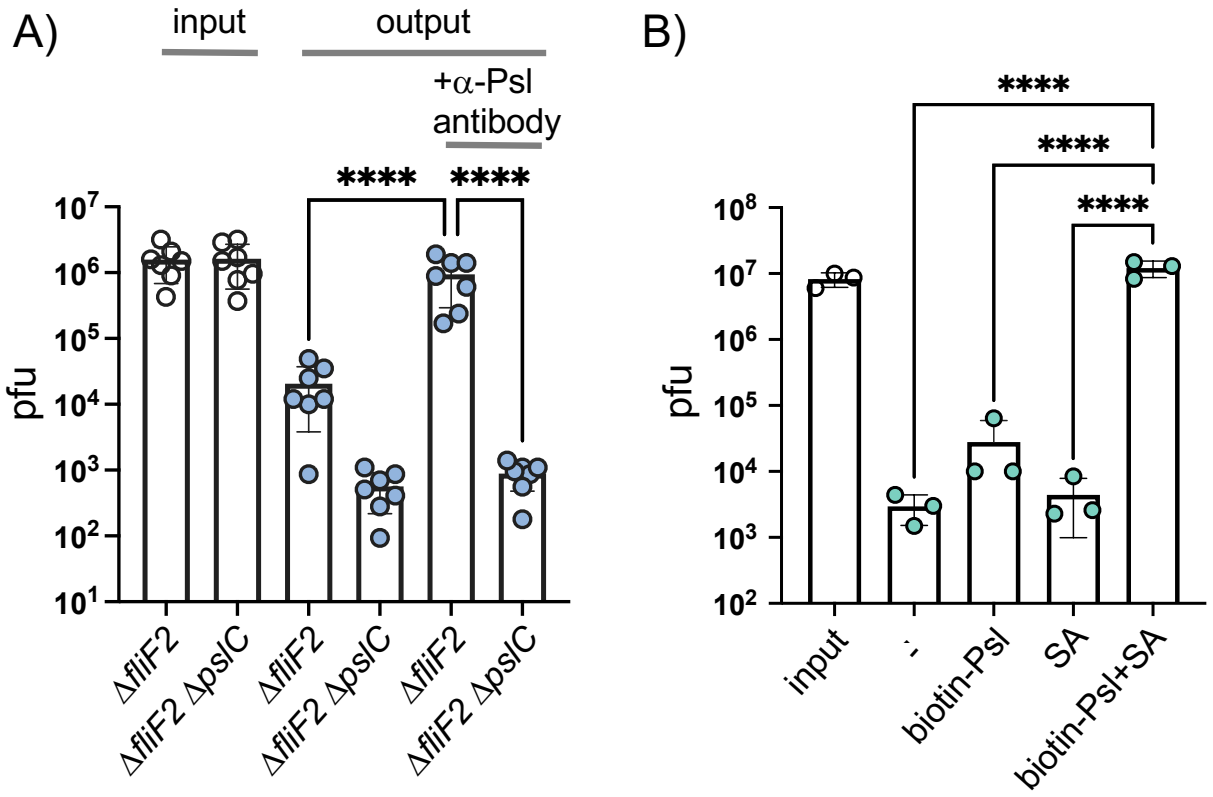

Fig. 4. Phage Clew-1 binds to Psl. A) Sterile filtered mid-log culture supernatants of PAO1F Δ*fliF2* or PAO1F Δ*fliF2* Δ*pslC* were incubated with phage Clew-1, as well as magnetic protein-A beads and, where indicated, a rabbit, anti-Psl antiserum. Beads were collected, washed 3x, and phage in the input and output samples were quantified by qPCR (7 independent replicates.) B) Phage Clew-1 was incubated for 1h in SM buffer with affinity purified, biotinylated Psl (biotin-Psl) and magnetic protein A beads, or magnetic streptavidin beads (SA), where indicated. Beads were collected and washed 3x, and phage in the input and output samples were quantified by qPCR (3 independent replicates). Statistical significance was determined by ANOVA with Sidák post-hoc test (**** $p<0.0001$).

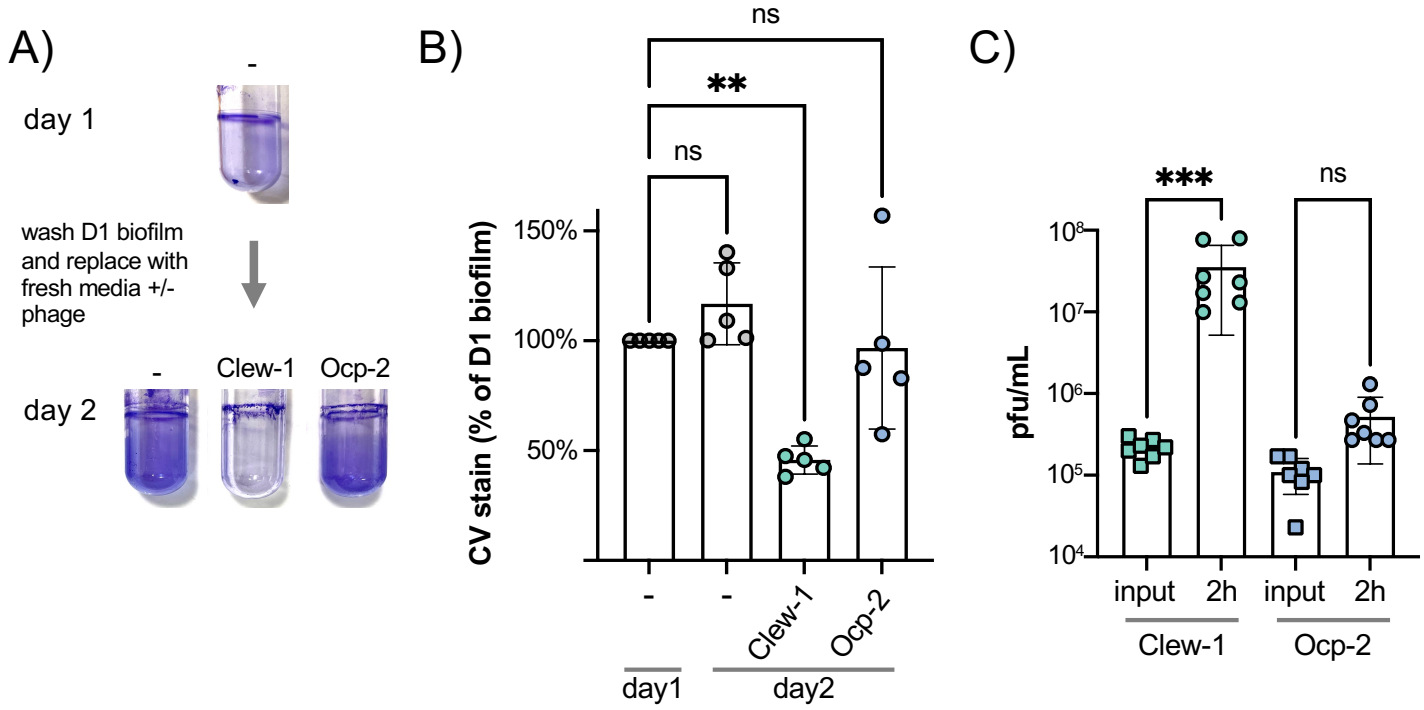

Fig. 5. Phage Clew-1 can infect *P. aeruginosa* in biofilms. A) Biofilms of wild type *P.* aeruginosa PAO1F were established overnight in 5mL culture tubes (1mL culture), the tubes were washed with PBS and 1.2mL LB, LB with 10^10 pfu phage Clew-1, or LB-with 10^10 pfu phage Ocp-2 were added back to each tube (1 was fixed with EtOH to represent the 1-day old biofilm). The following day all biofilms were washed with PBS and stained with crystal violet. B) PAO1F biofilms were established overnight in a 96-well plate (150µL of culture, 6 technical replicates/condition), washed and incubated overnight with 200µL of LB or LB with 10^9 pfu bacteriophage Clew-1 or Ocp-2. The biofilms were then washed, fixed, and stained with crystal violet, which was then solubilized with 30% acetic acid and quantified spectrophotometrically at 590 nm. The day 1 controls were set to 100% (5 biological replicates). C) Growth of phage Clew-1 or Ocp-2 was assayed by establishing a static biofilm in 5 mL culture tubes overnight (1mL culture volume). The biofilms were washed with PBS, then 1mL of LB with 10^5 pfu/mL of phage Clew-1 or Ocp-2 were added back. Biofilms were incubated at 37°C for 2h 15 minutes, the culture supernatants were filter sterilized and input and output phage concentrations were tittered (6 biological replicates). Statistical significance was determined by ANOVA with Šídák's multiple comparisons test test (** $p<0.01$, *** $p<0.001$).

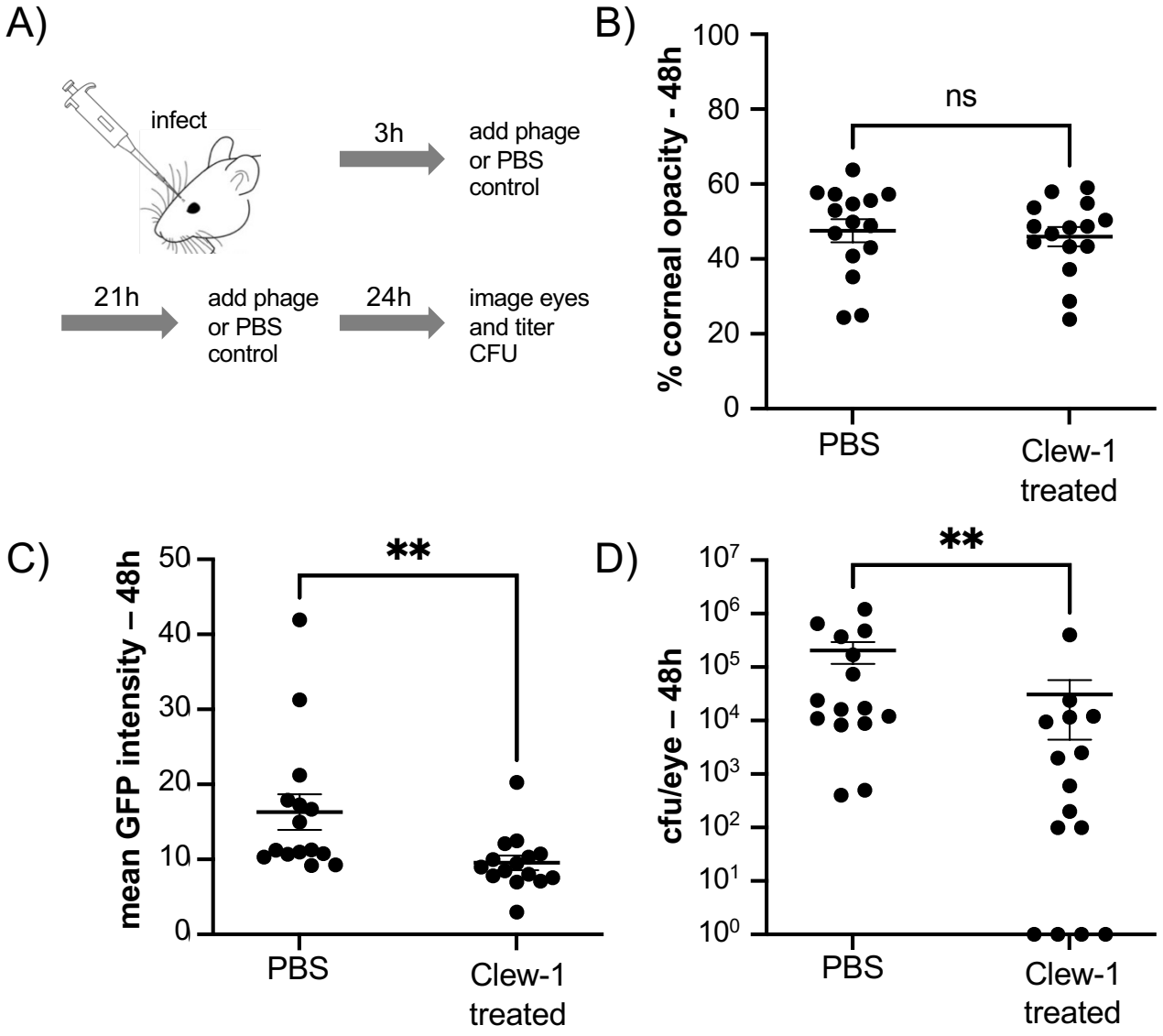

Fig. 6. Phage Clew-1 reduces the bacterial burden in a mouse cornea model of infection. A) Mice corneas were scratched and infected with 5*10^4 cfu strain PAO1F/pP25-GFPo, which produces GFP constitutively. Infected corneas were treated with 2*10^9 pfu phage Clew-1 or a PBS control at 3h and 24h post infection. B) At 48h post infection, the corneas were imaged by confocal microscopy to estimate the opacity (driven largely by the infiltration of neutrophils) and C) GFP fluorescence (produced by infecting *P. aeruginosa*). D) Eyes were also homogenized and plated for CFU to determine the total bacterial burden at the end of the experiment. Significance was determined by Mann-Whitney test (** $p<0.01$, n.s. not significant).